

Video Article

Facial Nerve Axotomy in Mice: A Model to Study Motoneuron Response to Injury

Deborah N. Olmstead^{1,2}, Nichole A. Mesnard-Hoaglin³, Richard J. Batka^{1,2}, Melissa M. Haulcomb^{1,2}, Whitney M. Miller^{1,2}, Kathryn J. Jones^{1,2}¹Anatomy and Cell Biology, Indiana University School of Medicine²Research and Development Services, Richard L. Roudebush VA Medical Center³Department of Anatomy and Cell Biology, University of Illinois, ChicagoCorrespondence to: Kathryn J. Jones at kjones1@iupui.eduURL: <http://www.jove.com/video/52382>DOI: [doi:10.3791/52382](https://doi.org/10.3791/52382)

Keywords: Neuroscience, Issue 96, Neuroscience, neuron, motoneuron, mouse, axotomy, facial nerve, crush, nerve injury, nerve regeneration

Date Published: 2/23/2015

Citation: Olmstead, D.N., Mesnard-Hoaglin, N.A., Batka, R.J., Haulcomb, M.M., Miller, W.M., Jones, K.J. Facial Nerve Axotomy in Mice: A Model to Study Motoneuron Response to Injury. *J. Vis. Exp.* (96), e52382, doi:10.3791/52382 (2015).

Abstract

The goal of this surgical protocol is to expose the facial nerve, which innervates the facial musculature, at its exit from the stylomastoid foramen and either cut or crush it to induce peripheral nerve injury. Advantages of this surgery are its simplicity, high reproducibility, and the lack of effect on vital functions or mobility from the subsequent facial paralysis, thus resulting in a relatively mild surgical outcome compared to other nerve injury models. A major advantage of using a cranial nerve injury model is that the motoneurons reside in a relatively homogenous population in the facial motor nucleus in the pons, simplifying the study of the motoneuron cell bodies. Because of the symmetrical nature of facial nerve innervation and the lack of crosstalk between the facial motor nuclei, the operation can be performed unilaterally with the unaxotomized side serving as a paired internal control. A variety of analyses can be performed postoperatively to assess the physiologic response, details of which are beyond the scope of this article. For example, recovery of muscle function can serve as a behavioral marker for reinnervation, or the motoneurons can be quantified to measure cell survival. Additionally, the motoneurons can be accurately captured using laser microdissection for molecular analysis. Because the facial nerve axotomy is minimally invasive and well tolerated, it can be utilized on a wide variety of genetically modified mice. Also, this surgery model can be used to analyze the effectiveness of peripheral nerve injury treatments. Facial nerve injury provides a means for investigating not only motoneurons, but also the responses of the central and peripheral glial microenvironment, immune system, and target musculature. The facial nerve injury model is a widely accepted peripheral nerve injury model that serves as a powerful tool for studying nerve injury and regeneration.

Video Link

The video component of this article can be found at <http://www.jove.com/video/52382/>

Introduction

Many peripheral nerve injury models exist, but one that stands out for the study of motoneurons is the facial nerve axotomy model. The facial nerve, also known as cranial nerve VII, originates in the pons and innervates the muscles of facial expression^{1,2}. In this surgical protocol, the facial nerve is exposed at its exit from the stylomastoid foramen and either cut or crushed. The severity of nerve injury can be classified following the Sunderland³ classifications, which differentiates the injury based on the intactness of the axons, endoneurium, perineurium, and epineurium, which are connective tissue layers that sequentially wrap around the axon bundles. In the crush injury (axonotmesis), the axons are severed, but the perineurium and epineurium are preserved. Complete functional recovery from facial nerve crush occurs in about 11 days because the intact nerve sheath serves as a conduit within which the axons regrow^{4,5}. On the other hand, in the cut injury (neurotmesis), the axons and all 3 connective tissue layers are severed, and the entire distal nerve must regrow to restore musculature innervation. Surgical reconnection of the epineurium is often performed in human patients with nerve transection injuries, however the recovery outcomes are seldom optimal. Further study is required to understand why the nerve fails to regrow to its target and what therapies can be employed to improve and accelerate the regenerative process.

There are many advantages to studying nerve injury using the facial nerve axotomy model. First, the facial nerve axotomy procedure is quick, easy, and highly reproducible; and the resultant paralysis of the facial muscles does not impact vital functions and is well tolerated by the animal. Because this is a cranial nerve injury model, studying the motoneuron cell bodies is simplified because the motoneurons reside in a relatively homogenous population in the facial motor nucleus in the pons. The population does differ based on the subnuclear pattern within the facial motor nucleus, as there are seven subnuclei each specific to innervating a specific group of muscles, so subnuclear differences in response to axotomy may impact results^{2,6,7}.

A major benefit of the facial nerve injury model is that the unaxotomized side can serve as a paired internal control because the nerve innervation is highly symmetrical and there is no crosstalk between the facial motor nuclei⁸. Another advantage of using this surgical method is

the lack of direct trauma to the CNS or disruption of the blood brain barrier⁹. Complications such as excessive bleeding and infection are rare with this procedure.

A variety of analyses can be performed to assess the physiologic response to nerve injury. The recovery of the eye blink reflex and whisker activity can be used as a behavioral measure of functional recovery^{10,11}. Video recording of vibrissae activity is currently the most powerful method for detecting recovery of facial nerve innervation^{12,13}. After euthanasia, histological analysis of the brainstem can be performed on the motoneuron cell bodies within the facial motor nucleus. The facial motor nucleus is subdivided into seven subnuclei, each specific to certain facial muscles, allowing for differential examination of responses to injury^{2,6}. Facial motoneurons can be counted to quantify cell survival, or immunohistochemistry can be used to identify biomarkers and specific cell populations¹⁴. The facial motor nucleus can be accurately microdissected using laser capture for molecular analysis of the cellular response to nerve injury^{15,16}. Impacts of the facial nerve axotomy can be analyzed in the motor cortex^{17,18}. Also, the nerve can be dissected to study Wallerian degeneration¹⁹ or axon regeneration²⁰, and the muscles can be removed to study neuromuscular junctions²¹. The facial nerve axotomy can also be used to study the accompanying central and peripheral glial cells²², target musculature²¹, and the immune system response²³. Although much has been accomplished in studying the facial nerve axotomy model²⁴, further study of peripheral nerve injury is required because nerve damage is a significant problem for patients and current treatments fail to produce optimal results. This model is a powerful tool for examining the physiologic response to nerve injury and analyzing the effectiveness of nerve regeneration therapies.

Protocol

All procedures executed are approved by the Indiana University School of Medicine Institutional Animal Care and Use Committee and follow National Institute of Health guidelines.

1. Surgical Technique

1. Maintain aseptic technique during this procedure by using sterile gloves, instruments, and a sterile surgical field according to NIH guidelines²⁵. Sterilize tools before beginning surgery by autoclaving them (see **Table of Specific Reagents/Equipment** for complete list). Use a glass bead sterilizer to sterilize tools during the operation.

2. Anesthesia and Preparation

1. Anesthetize the mouse in an anesthesia box with a mixture of 0.9 L/min oxygen and 2.5% isoflurane using a veterinary isoflurane vaporizer system. Ensure that the mouse does not respond to changes in body position before removing it from the box.
2. Apply ophthalmic ointment to the mouse's eyes to protect them from drying out.
3. Switch the gas flow from the box to the nose cone. Place the mouse squarely on its left side on a heated pad covered with a surgical pad and absorbent bench paper with its nose and mouth inside the cone. Continuously monitor the mouse's breathing rhythm and rate and adjust isoflurane levels as needed (between 2.5 - 3% isoflurane) to maintain an adequate level of anesthesia, and use the toe pinch reflex to confirm total sedation.

3. Surgical Approach

1. Align and focus the stereoscope with the surgical field. Adjust the nose cone and tape it down so that it is positioned along the edge of the visual field.
2. With the mouse lying on its left side, tape the edge of the right ear to the nose cone, exposing the area behind the ear where the incision will be made. Ensure that the posterior auricular vein travels horizontally across the ear. Note that the correct placement of the animal and taping of the ear are crucial in order to quickly find the facial nerve.
3. Wet the fur on and behind the ear with 70% ethanol and shave the surgical site using a razor or scalpel blade. Pre-wetting the fur makes shaving easier in this anatomical location.
4. Clean the skin with an iodine solution, such as Betadine surgical scrub (7.5% povidone-iodine), followed by 70% ethanol. Repeat this cleaning two more times to thoroughly disinfect the area.
5. To determine where to make the incision, trace the posterior auricular vein from the ear caudally to the area posterior to the ear protuberance. Using spring scissors, make a 4 mm incision 2 - 3 mm posterior to the protuberance.
6. Dissect through the subcutaneous fat and fascia using blunt dissection. Avoid direct cutting with the scissors because blood vessels or muscle tissue could be easily damaged.
7. If bleeding occurs, apply pressure to the surgical site with a sterile cotton swab for at least 30 sec. If significant fluid loss occurs, inject the mouse intraperitoneally with up to 0.5 ml of sterile 0.9% saline solution using a 25 or 27 G needle.
8. Use several key landmarks, the spinal accessory nerve, ear canal, and anterior digastric muscle (described below), to locate the facial nerve. Dissect around these landmarks until the branches of the facial nerve are visualized. The nerve will appear as a significant solid white structure when it is revealed and a layer of fascia adheres it to the underlying structures.
 1. Find the spinal accessory nerve, which travels from the caudal portion of the skull to innervate the trapezius muscle, once the subcutaneous fat and fascia have been dissected. The facial nerve is deep to the spinal accessory nerve.
 2. Find the cartilaginous ear canal that looks pearly white and can be seen rostral to the facial nerve.
 3. Find the muscle belly of the anterior digastric muscle that lies on top of and caudal to the facial nerve.
9. When the main branches of the facial nerve are visualized, trace them dorsally to find their origin from the stylomastoid foramen. Using fine tipped Dumont forceps #5/45 to hold the surgical site open, advance the spring scissor tips following the nerve's path, then move the forceps dorsally to keep the newly advanced area open.
10. Visualize the trunk of the facial nerve with the zygomatic, buccal, and marginal mandibular branches at this point.

NOTE: The temporal branch will be found closer to the foramen. The marginal mandibular nerve branches into its upper and lower parts closer to the jaw, thus those nerve branches will not be visible at this level.

1. If performing a nerve transection, stabilize the nerve gently with the fine tip forceps and cut the nerve with the spring scissors. Avoid applying too much traction to the nerve with the forceps to prevent avulsing the nerve from the brainstem. Push the stumps away from each other, or cut and remove a portion of the distal nerve to ensure that no reconnection can occur.
2. If performing a crush injury, use Dumont #5/45 forceps to compress the nerve for 30 sec using constant pressure to sever all axons, then repeat this crush at a second angle perpendicular to the first crush site. Avoid applying variable amounts of pressure during the 30 sec crush, otherwise the injury will be inconsistent between animals.

4. Closing and Recovery

1. Reposition the fat and muscles over the underlying structures.
2. Approximate the edges of the incision and close the wound using a 7.5 mm wound clip. Sutures or glue are also acceptable for wound closure. Postsurgical analgesics can be provided at this time.
3. Remove the tape from the mouse's ear. Turn off the isoflurane flow and allow the mouse to breathe pure oxygen for 30 sec to 1 min. Place the mouse in an empty cage with no bedding to recover from anesthesia.
4. When the mouse is recovered, examine its behavior for confirmatory signs of facial paralysis. The whiskers will be paralyzed and angled back towards the cheek, the nose will be deviated, and the eye will not blink in response to a puff of air.
5. House animals jointly after surgery if they are female. Avoid housing male mice jointly because they are more aggressive and tend to forcibly remove their cagemate's wound clips, which leads to infection. Provide postsurgical analgesics at this time, if necessary.
6. Monitor the mice once a day for several days after the operation to ensure that no infection or other complication occurs postoperatively. Remove wound clips 7 - 10 days after the surgery if they have not fallen out on their own.
7. Apply lubricating eye ointment to the affected eye daily to prevent corneal complications, either until the eye blink reflex is recovered or until euthanasia.

Representative Results

After the facial nerve axotomy is performed, motoneuron loss occurs as a result of the injury. Motoneuron survival after injury depends on many variables, such as gender, animal age at time of surgery, and the timepoint at which the motoneuron counts are done, and the Moran and Graeber review²⁴ and Jinno and Yamada review²² both summarize motoneuron survival data. Typically, about 86% of motoneurons survive at 28 days post-axotomy^{14,15,26}. Kinetics of motoneuron loss are described in Serpe *et al.* 2000. **Figure 1** illustrates the variation in motoneuron survival in multiple genetically modified mice. No significant differences are observed in facial motoneuron counts of the control side, indicating that the genetic alterations do not impact baseline counts. Compared to the motoneuron survival in wild type mice ($84\% \pm 2.0$; **Figure 1A,D**), significant cell loss is observed in a mouse model of amyotrophic lateral sclerosis (SOD1^{G93A}; $68\% \pm 1$; **Figure 1B,E**) as well as the immunodeficient recombination-activating gene-2 knockout mouse (RAG-2^{-/-}; $57\% \pm 2.5$; **Figure 1C,F**)²⁷.

Figure 2 demonstrates the laser capture microdissection technique applied to the facial motor nucleus. The entire facial motor nucleus can be captured (**Figure 2A-C**), or subnuclei can be collected separately (**Figure 2D-F**). For greater precision, motoneurons can be captured individually, and the remaining neuropil can be collected for analysis (**Figure 2G-I**). **Figure 3** depicts qPCR results of the RNA material extracted from the subnuclear samples comparing the ventromedial and ventrolateral subnuclei. The four genes tested, β _{II} *tubulin*, growth associated protein-43 (*Gap-43*), hemopoietic- and neurologic-expressed sequence-1 (*Hn1*), and brain-derived neurotrophic factor (*BDNF*) are all associated with the nerve regeneration response and there are interesting differences between the two subnuclei and their gene expression profiles after axotomy¹⁶.

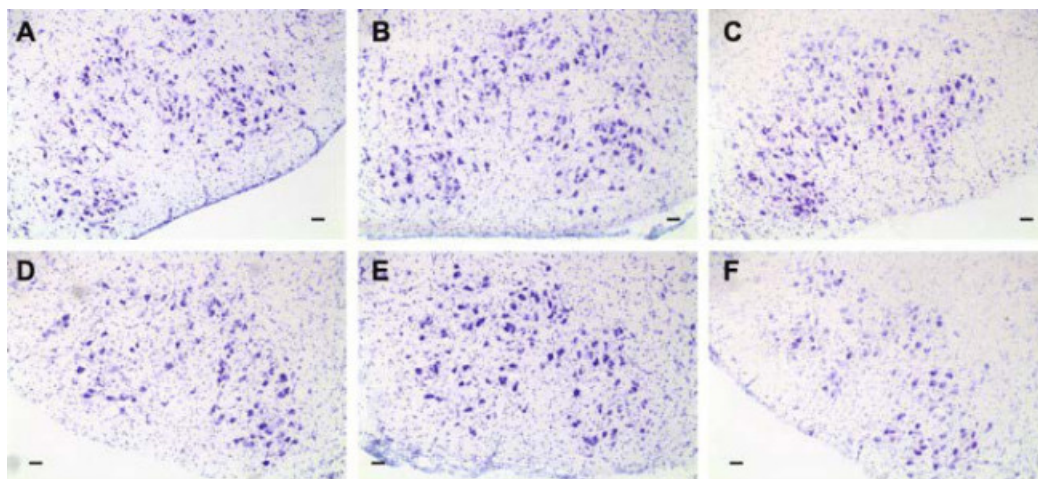


Figure 1. Representative coronal facial motor nucleus sections stained with thionin and quantified 28 days after facial nerve transection. Facial motor nuclei are shown from (A,D) WT, (B,E) SOD1^{G93A}, and (C,F) RAG-2^{-/-} mice (control side, axotomized side). Scale bars = 120 μ m. This figure has been modified from²⁷. Please click here to view a larger version of this figure.

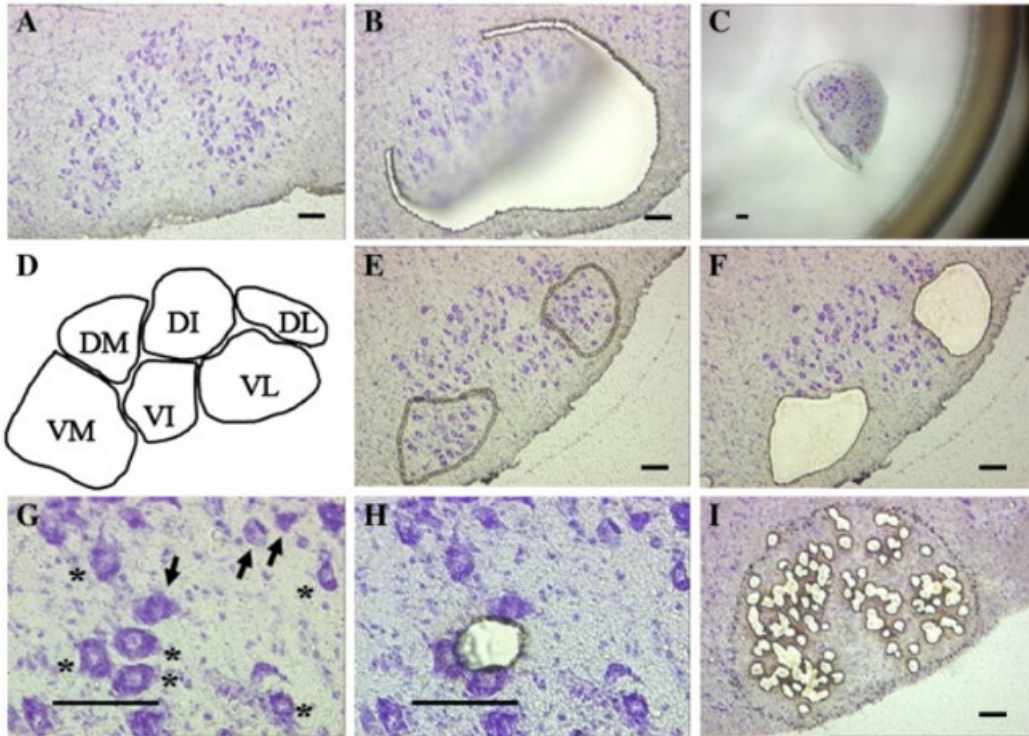


Figure 2. Laser microdissection of the facial motor nucleus. (A) Thionin-stained section of axotomized facial nucleus, (B) with partial laser microdissection of the axotomized facial nucleus, and (C) collection of laser microdissected tissue. A template (D) of the subnuclei was superimposed on the computer screen to identify the ventromedial and ventrolateral facial subnuclei for laser microdissection (E,F). Facial motoneurons were laser microdissected based on their morphology with a visible nucleus and nucleolus (* indicates motoneuron, G,H), while FMN cell body fragments, indicated by the arrows (G), were laser microdissected separately and disposed of to eliminate FMN mRNA in the neuropil samples. After all FMN and cell body fragments were collected, the remaining facial nucleus tissue was laser microdissected as the neuropil sample (I). Scale bars = 100 μ m. This figure has been modified from ¹⁶. [Please click here to view a larger version of this figure.](#)

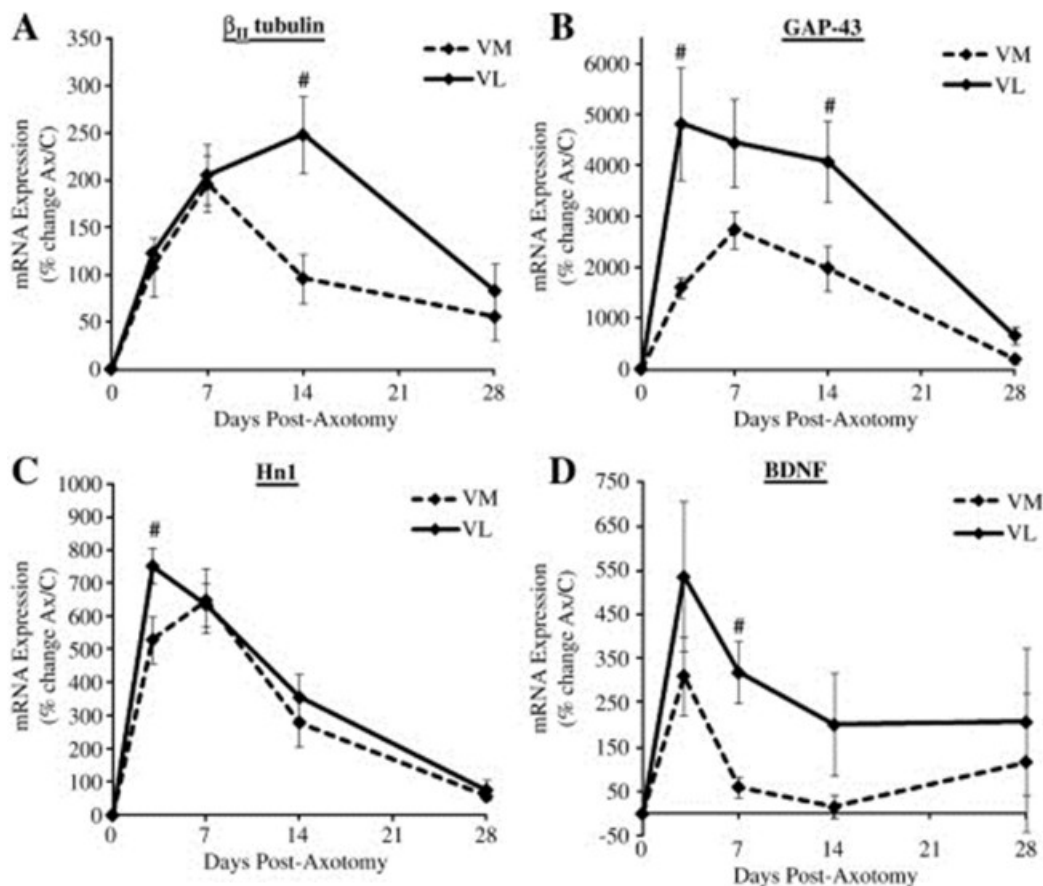


Figure 3. Pro-regeneration and pro-survival mRNA expression in the ventromedial (VM) and ventrolateral (VL) facial motor subnuclear regions following facial nerve axotomy. Average percent of mRNA expression \pm SEM in the transected VM and VL facial subnuclei relative to the unoperated control subnuclei (A-D). Time-course of mRNA expression includes no injury (0), 3, 7, 14, and 28 dpo for β II tubulin (A), GAP-43 (B), Hn1 (C), and BDNF (D). # represents significant differences of VL compared to VM, at $p < 0.05$. This figure has been modified from ¹⁶.

Discussion

The critical step for this protocol is positioning the mouse properly before surgery is begun. If the mouse is not lying flat on its side, the ear is not taped at the correct angle, or the incision is made in an incorrect location, then finding the facial nerve becomes much more difficult. When this technique is mastered, surgeries will take only minutes per mouse.

Either sutures, glue, or wound clips can be used to close the wound. Wound clips are preferred because of the small size of incision and rapidity with which they can be applied. We have determined that if wound clips are used and the mice are housed together, female mice fare better than male mice because males housed together often remove their cagemate's wound clips, leading to infection of the surgical site.

Modifications can be made to the injury, such as changing the location along the nerve to induce injury. For example, the injury could be administered along one of the branches of the facial nerve²⁸, or the skull could be opened to deliver an intracranial injury²⁹. In addition, a variety of treatments can be implemented, such as applying drugs to the nerve stump¹⁴, injecting medicines systemically³⁰, or even performing cell transfers³¹. Motoneuron diseases such as amyotrophic lateral sclerosis can also be studied using the facial nerve axotomy model³². Ongoing applications of this technique involve studying nerve reconnection strategies after transection and the application of pharmaceutical agents to accelerate nerve regeneration after injury.

One of the most useful aspects of this surgery is that it is easy to confirm successful axotomy by monitoring the mouse's vibrissae orientation and movements as well as the eye blink reflex.

The paralysis does not affect the animal's vital functions and overall is well tolerated in the mouse.

A major advantage of the facial nerve injury model is that the isolated study of motoneurons is possible. However, because this is a cranial nerve injury, results found using this method may not translate to spinal, autonomic, or sensory nerve injury models. To study these other nerve injury types, a sciatic³³ or tibial³⁴ nerve injury model is recommended. The drawback of these models is that there is crosstalk from the contralateral neurons in the spinal cord that can confound results. There is no crosstalk between the facial motor nuclei, so the contralateral facial motor nucleus can serve as a paired internal control. The facial nerve axotomy model presents many advantages for studying nerve injury and regeneration.

Disclosures

The authors have nothing to disclose.

Acknowledgements

This work is funded by NIH RO1 NS 40433 (K.J.J.).

References

1. Kaufman, M., & Bard, J. *The Anatomical Basis of Mouse Development*. Elsevier, New York, NY (1999).
2. Ashwell, K. The adult mouse facial nerve nucleus: morphology and musculotopic organization. *Journal of Anatomy*. **135**, 531-538 (1982).
3. Sunderland, S. A classification of peripheral nerve injuries producing loss of function. *Brain : A Journal Of Neurology*. **74**, 491-516 (1951).
4. Beahrs, T., Tanzer, L., Sanders, V. M., & Jones, K. J. Functional recovery and facial motoneuron survival are influenced by immunodeficiency in crush-axotomized mice. *Experimental Neurology*. **221**, 225-230, doi: 10.1016/j.expneurol.2009.11.003 (2010).
5. Mesnard, N. A., Haulcomb, M. M., Tanzer, L., Sanders, V., & Jones, K. J. Delayed functional recovery in presymptomatic mSOD1G93A mice following facial nerve crush axotomy. *Journal of Neurodegeneration & Regeneration*. **4**, 21-25 (2013).
6. Komiyama, M., Shibata, H., & Suzuki, T. Somatotopic representation of facial muscles within the facial nucleus of the mouse. A study using the retrograde horseradish peroxidase and cell degeneration techniques. *Brain Behav Evol*. **24**, 144-151, doi: 10.1159/000121312 (1984).
7. Canh, M. Y., Serpe, C. J., Sanders, V., & Jones, K. J. CD4(+) T cell-mediated facial motoneuron survival after injury: Distribution pattern of cell death and rescue throughout the extent of the facial motor nucleus. *Journal of Neuroimmunology*. **181**, 93-99, doi: 10.1016/j.jneuroim.2006.08.006 (2006).
8. Isokawa-Akesson, M., & Komisaruk, B. Difference in projections to the lateral and medial facial nucleus: anatomically separate pathways for rhythmic vibrissa movement in rats. *Exp Brain Res*. **65**, 385-398 (1987).
9. Streit, W., & Kreutzberg, G. Response of endogenous glial cells to motor neuron degeneration induced by toxic ricin. *The Journal of Comparative Neurology*. **268**, 248-263, doi: 10.1002/cne.902680209 (1988).
10. Serpe, C. J., Tetzlaff, J. E., Coers, S., Sanders, V., & Jones, K. J. Functional recovery after facial nerve crush is delayed in severe combined immunodeficient mice. *Brain, Behavior, And Immunity*. **16**, 808 - 812, doi: 10.1016/S0889-1591(02)00017-X (2002).
11. Lal, D. *et al.* Electrical stimulation facilitates rat facial nerve recovery from a crush injury. *Otolaryngology--Head And Neck Surgery : Official Journal Of American Academy Of Otolaryngology-Head And Neck Surgery*. **139**, 68-73, doi: 10.1016/j.otohns.2008.04.030 (2008).
12. Tomov, T. *et al.* An Example of Neural Plasticity Evoked by Putative Behavioral Demand and Early Use of Vibrissal Hairs after Facial Nerve Transection. *Experimental Neurology*. **178**, 207-218, doi: 10.1006/exnr.2002.8040 (2002).
13. Skouras, E., & Angelov, D. N. Experimental studies on post-transectional facial nerve regrowth and functional recovery of paralyzed muscles of the face in rats and mice. *Anatomy (International Journal of Experimental and Clinical Anatomy)*. **4**, 1-27, doi: 10.2399/ana.10.002 (2010).
14. Xin, J. *et al.* IL-10 within the CNS is necessary for CD4+ T cells to mediate neuroprotection. *Brain, Behavior, And Immunity*. **25**, 820-829, doi: 10.1016/j.bbi.2010.08.004 (2011).
15. Mesnard, N. A., Sanders, V. M., & Jones, K. J. Differential gene expression in the axotomized facial motor nucleus of presymptomatic SOD1 mice. *The Journal of Comparative Neurology*. **519**, 3488-3506, doi: 10.1002/cne.22718 (2011).
16. Mesnard, N. A., Alexander, T. D., Sanders, V. M., & Jones, K. J. Use of laser microdissection in the investigation of facial motoneuron and neuropil molecular phenotypes after peripheral axotomy. *Experimental Neurology*. **225**, 94-103, doi: 10.1016/j.expneurol.2010.05.019 (2010).
17. Franchi, G. Changes in motor representation related to facial nerve damage and regeneration in adult rats. *Experimental Brain Research*. **135**, 53-65, doi: 10.1007/s002210000503 (2000).
18. Munera, A., Cuestas, D. M., & Troncoso, J. Peripheral facial nerve lesions induce changes in the firing properties of primary motor cortex layer 5 pyramidal cells. *Neuroscience*. **223**, 140-151, doi: 10.1016/j.neuroscience.2012.07.063 (2012).
19. Liu, L. *et al.* Hereditary absence of complement C5 in adult mice influences Wallerian degeneration, but not retrograde responses, following injury to peripheral nerve. *Journal of the Peripheral Nervous System*. **4**, 123-133 (1999).
20. Ferri, C., Moore, F., & Bisby, M. Effects of facial nerve injury on mouse motoneurons lacking the p75 low-affinity neurotrophin receptor. *Journal of Neurobiology*. **34**, 1-9, doi: 10.1002/(SICI)1097-4695(199801)34 (1997).
21. Zhou, R. Y., Xu, J., Chi, F. L., Chen, L. H., & Li, S. T. Differences in sensitivity to rocuronium among orbicularis oris muscles innervated by normal or damaged facial nerves and gastrocnemius muscle innervated by somatic nerve in rats: combined morphological and functional analyses. *The Laryngoscope*. **122**, 1831-1837, doi: 10.1002/lary.23286 (2012).
22. Jinno, S., & Yamada, J. Using comparative anatomy in the axotomy model to identify distinct roles for microglia and astrocytes in synaptic stripping. *Neuron Glia Biology*. **7**, 55-66, doi: 10.1017/S1740925X11000135 (2011).
23. Jones, K. J., Serpe, C. J., Byram, S. C., Deboy, C. A., & Sanders, V. M. Role of the immune system in the maintenance of mouse facial motoneuron viability after nerve injury. *Brain, Behavior, And Immunity*. **19**, 12-19, doi: 10.1016/j.bbi.2004.05.004 (2005).
24. Moran, L. B., & Graeber, M. B. The facial nerve axotomy model. *Brain research. Brain research reviews*. **44**, 154-178, doi: 10.1016/j.brainresrev.2003.11.004 (2004).
25. Council, N. R. *Guide for the Care and Use of Laboratory Animals: Eighth Edition*. The National Academies Press, New York, NY (2011).
26. Serpe, C. J., Kohm, A. P., Huppenbauer, C. B., Sanders, V., & Jones, K. J. Exacerbation of Facial Motoneuron Loss after facial nerve transection in severe combined immunodeficient (scid) mice. *Neuroscience*. **19** (1999).
27. Mesnard-Hoaglin, N. A. *et al.* SOD1(G93A) transgenic mouse CD4(+) T cells mediate neuroprotection after facial nerve axotomy when removed from a suppressive peripheral microenvironment. *Brain, Behavior, And Immunity*. **40**, 55-60, doi: 10.1016/j.bbi.2014.05.019 (2014).
28. Wang, H. *et al.* Establishment and assessment of the perinatal mouse facial nerve axotomy model via a subauricular incision approach. *Experimental Biology And Medicine*. **237**, 1249-1255, doi: 10.1258/ebm.2012.012134 (2012).
29. Sharma, N., Moeller, C. W., Marzo, S. J., Jones, K. J., & Foecking, E. M. Combinatorial treatments enhance recovery following facial nerve crush. *The Laryngoscope*. **120**, 1523-1530, doi: 10.1002/lary.20997 (2010).

30. Lieberman, D. M., Jan, T. A., Ahmad, S. O., & Most, S. P. Effects of corticosteroids on functional recovery and neuron survival after facial nerve injury in mice. *Archives of Facial Plastic Surgery*. **13**, 117-124, doi: 10.1001/archfacial.2010.98 (2011).
31. Serpe, C. J., Coers, S., Sanders, V. M., & Jones, K. J. CD4+ T, but not CD8+ or B, lymphocytes mediate facial motoneuron survival after facial nerve transection. *Brain, Behavior, And Immunity*. **17**, 393-402, doi: 10.1016/s0889-1591(03)00028-x (2003).
32. Haulcomb, M. M. *et al.* Axotomy-induced target disconnection promotes an additional death mechanism involved in motoneuron degeneration in ALS transgenic mice. *The Journal of Comparative Neurology*. doi: 10.1002/cne.23538 (2014).
33. Bauder, A. R., & Ferguson, T. A. Reproducible mouse sciatic nerve crush and subsequent assessment of regeneration by whole mount muscle analysis. *Journal of Visualized Experiments : JoVE*. (60), doi: 10.3791/3606 (2012).
34. Richner, M., Bjerrum, O. J., Nykjaer, A., & Vaegter, C. B. The spared nerve injury (SNI) model of induced mechanical allodynia in mice. *Journal of Visualized Experiments : JoVE*. (54), doi: 10.3791/3092 (2011).